ANTIOXIDANTS & REDOX SIGNALING
Volume 11, Number 7, 2009

DOI: 10.1089/ars.2008.2420

Original Research Communication

Structural and Functional Characterization of the Oxidoreductase α-DsbA1 from *Wolbachia pipientis*

Mareike Kurz,[1] Iñaki Iturbe-Ormaetxe,[2] Russell Jarrott,[1] Stephen R. Shouldice,[1] Merridee A. Wouters,[3] Patrick Frei,[4] Rudi Glockshuber,[4] Scott L. O'Neill,[2] Begoña Heras,[1] and Jennifer L. Martin[1]

Abstract

The α-proteobacterium *Wolbachia pipientis* is a highly successful intracellular endosymbiont of invertebrates that manipulates its host's reproductive biology to facilitate its own maternal transmission. The fastidious nature of *Wolbachia* and the lack of genetic transformation have hampered analysis of the molecular basis of these manipulations. Structure determination of key *Wolbachia* proteins will enable the development of inhibitors for chemical genetics studies. *Wolbachia* encodes a homologue (α-DsbA1) of the *Escherichia coli* dithiol oxidase enzyme EcDsbA, essential for the oxidative folding of many exported proteins. We found that the active-site cysteine pair of *Wolbachia* α-DsbA1 has the most reducing redox potential of any characterized DsbA. In addition, *Wolbachia* α-DsbA1 possesses a second disulfide that is highly conserved in α-proteobacterial DsbAs but not in other DsbAs. The α-DsbA1 structure lacks the characteristic hydrophobic features of EcDsbA, and the protein neither complements EcDsbA deletion mutants in *E. coli* nor interacts with EcDsbB, the redox partner of EcDsbA. The surface characteristics and redox profile of α-DsbA1 indicate that it probably plays a specialized oxidative folding role with a narrow substrate specificity. This first report of a *Wolbachia* protein structure provides the basis for future chemical genetics studies. *Antioxid. Redox Signal.* 11, 1485–1500.

Introduction

Wolbachia pipientis is one of the most successful endosymbionts yet described, infecting huge numbers of insects, spiders, mites, and filarial nematodes (31, 49). This gram-negative α-proteobacterium lives inside a vacuole of host origin, mainly in reproductive tissues, where it induces a variety of host phenotypes—including feminization, cytoplasmic incompatibility, parthenogenesis, and male killing—that increase the proportion of infected females in the host population, thereby favoring *Wolbachia*'s own maternal transmission (56). How *Wolbachia* induces these phenotypes is the subject of intense research because *Wolbachia*-induced traits can potentially be used to control insect pest populations and mosquito-borne diseases such as malaria and Dengue fever (7, 42).

The lack of technologies to culture and transform *Wolbachia* makes it a difficult organism to study. Recent advances suggest that proteins secreted from *Wolbachia* are responsible for the phenotypic changes observed in their hosts (30), although it is not known how secreted proteins traverse the host vacuolar membrane that surrounds the bacteria. The cysteines in secreted proteins form disulfide bonds that stabilize these proteins in the extracellular environment. Most organisms encode elaborate machinery to catalyze this oxidative folding step (22). Cytoplasmic proteins, conversely, most often have their cysteine residues in the reduced or thiol form. Although *Wolbachia pipientis w*Mel infecting *Drosophila melanogaster* is an intracellular organism, its genome (58) encodes three predicted periplasmic proteins homologous to proteins of the *E. coli* oxidative folding machinery. Given that the function of these disulfide-forming proteins could be involved in

[1]Institute for Molecular Bioscience, and [2]School of Biological Sciences, The University of Queensland, Brisbane, Queensland; [3]Victor Chang Cardiac Research Institute and School of Medical Sciences, University of New South Wales, Sydney, Australia.
[4]Institute for Molecular Biology and Biophysics, Zürich, Switzerland.

Table 1. Sequence Characteristics of Putative DsbA Homologues across Proteobacteria

Taxonomic group	*No. seqs*	*No. genera*	*No. species*	*Res range of pred. mature proteins*	*X of CXHC motif*	*Residue before cisPro*[g]	*Additional conserved residues*[i]	*Name*
α-Proteobacteria	60	34	57[a]	196–282[e]	P/A/V/G/S/M/Y/T	T	I/L/V–10, Y/F–5, S/A–3, V/I+16, R/K+26, C+43-45, C+92-105	α-DsbA
β-Proteobacteria	29	15	25[b]	201–232	P/I/V	V/T	Y/F-24-26, I/V–10, E/D–9, V–8, E–6, F/I–5, F–4, Y–2, W/F+73-87, S/A+91-105, G+120-134	β-DsbA
γ-Proteobacteria	60	33	51[c]	197–223[f]	P/Q/V/G/I/T	V[h]	L/V–8, E–6, F–5, I/V ~ +120, V/L ~ +150	γ-DsbA
ε-Proteobacteria	7	1	6[d]	212–223	P/I/T/Q	V/T	L–19, I/V–15, N–10, V/L–8, I/V–7, F–4, S–3, Y–2, Y+1, S+24-25, F+37-39, A+38-40, A ~ +139, F ~ +140	ε-DsbA

By using the EcDsbA protein sequence, the nonredundant (nr) database at NCBI was searched for putative DsbA homologues by using the PSI-BLAST algorithm (1). Putative DsbA homologues were selected from sequences originating from the phylum Proteobacteria and where the protein contained both a CXHC active-site motif and a *cis*Pro loop motif, and 159 sequences were found that matched these criteria. To identify conserved residues, sequence alignment of the DsbA homologues was performed by using ClustalW (12). The highest numbers of DsbA homologues were found in α, β, and γ-proteobacteria. [a]Fifty-four species encode one DsbA-homologue, three species encode two DsbA-homologues. [b]Twenty-two species encode a single DsbA-homologue, two species encode two DsbA-homologues, one species encodes three DsbA-homologues. [c]Forty-six species encode one DsbA-homologue, 1 species encodes two DsbA-homologues, four species encode three DsbA-homologues. [d]Six species encode one DsbA-homologue, one species encodes two DsbA-homologues.

[e]Exceptions: *Magnetospirillum magnetotacticum* MS-1 ZP_00209268.1, 166 residues; ZP_00339759.1, one of two DsbA homologues of *Rickettsia akari* str. Hartford, 318 residues.

[f]Exceptions: *Photobacterium profundum* SS9 YP_130338.1, 244 residues; NP_820887.1, 1 of three DsbA-homologues of *Coxiella burnetii* RSA 493, 252 residues; *Microbulbifer degradans* 2-40 ZP_00318381.1, 293 residues.

[g]Residue preceding V *cis*Pro or T*cis*Pro: α-DsbAs, A/S/G; β-DsbAs, G/S; γ-DsbAs, G/S (see also[8]); ε-DsbAs, G.

[h]Across the γ-proteobacteria, we found three DsbA homologues with an ATP *cis*Pro loop and six DsbA homologues with a GTP *cis*Pro loop.

[i]Numbers indicate the position relative to the CXHC motif (−, N-terminal; +, C-terminal). All 7 ε-DsbAs originate from the genus *Campylobacter*; their high sequence identities indicate recent speciation/duplication. Altogether, 23 additional conserved residues were found for the ε-DsbAs, but only those near the CXHC or *cis*Pro loop are shown here.

generating the *Wolbachia*-induced host phenotypes, we decided to investigate them further.

Most studies on bacterial disulfide-forming proteins have focused on *E. coli*. In this organism, the oxidation of cysteine thiols to disulfides is catalyzed in the periplasm by the strong oxidant EcDsbA, which is reoxidized by ubiquinone Q8 *via* EcDsbB (reviewed in ref. 43). Proofreading and repair of incorrect disulfides is performed by *E. coli* isomerases EcDsbC or EcDsbG, and these are kept in the catalytically active, reduced form by EcDsbD (43). Dsb proteins generally incorporate a thioredoxin (TRX) fold with an active site formed from a CXXC redox motif, which can interconvert between disulfide and dithiol forms, and an adjacent *cis*-proline (*cis*-Pro) loop (40).

In *Wolbachia*, two of the three Dsb proteins are DsbA-like (α-DsbA1 and α-DsbA2) (35); the third protein is a putative DsbB (α-DsbB). No proteins encoding the DsbC-DsbD isomerase machinery, required for disulfide shuffling in *E. coli*, have been found in the *Wolbachia pipientis w*Mel genome. We aimed to investigate the structure and function of these proteins to confirm their role in disulfide catalysis. We originally identified α-DsbA1 from a bioinformatic analysis of proteobacterial DsbAs. *Wolbachia pipientis w*Mel α-DsbA1 is representative of a class of DsbAs that we named the α-DsbAs, because they are primarily found in α-Proteobacteria. The α-DsbAs differ from γ-DsbAs, characterized by the γ-proteobacterial *E. coli* EcDsbA, in that α-DsbA sequences are generally longer (~196–282 residues compared with ~197–223 residues) and have four rather than two conserved cysteines (Table 1). The high degree of conservation of the two additional cysteines in the α-DsbA sequences suggested that they might form a second disulfide. Furthermore, we found that the residue preceding the conserved proline in the *cis*Pro loop is an invariant Thr in α-DsbAs, whereas in γ-DsbAs like EcDsbA, this residue is a highly conserved Val (Table 1). Curiously, a Thr at this same position is characteristic of disulfide isomerases such as EcDsbC and EcDsbG (25). Given the lack of encoded disulfide isomerases in *Wolbachia pipientis w*Mel, we wondered whether the redox properties of α-DsbA1 might overlap with those of disulfide isomerases.

To investigate the role of α-DsbAs further, we characterized the structure and function of *Wolbachia pipientis w*Mel α-DsbA1 (WD1055 in the *w*Mel genome) and two variants that we designed to investigate the effect of (a) the Thr preceding the *cis*Pro loop, and (b) the second disulfide. To our knowledge, this is the first comprehensive structural and functional study of any *Wolbachia* protein.

Materials and Methods

Protein expression and purification

α-DsbA1 was expressed and purified as described previously (35). Mutagenesis of wt α-DsbA1 to α-DsbA1CA and α-DsbA1TV was performed by using the QuikChange II

Table 2. Primers Used for the Mutagenesis of *Wolbachia* αDsbA1

Primer	*Mutation*	*Sequence (5′–3′), mutation site is underlined, and the mutated bases shown in bold*
WCA1F	C97A	CTGCAATGCTAAGTCAT**GC**CTACGAAAAACAAGAAG
WCA1R	C97A	CTTCTTGTTTTTCGTAG**GC**ATGACTTAGCATTGCAG
WCA2F	C146A	GATGCATTTAACCAA**GC**CATTAATGATAAGAAAATAATG
WCA2R	C146A	CATTATTTTCTTATCATTAATG**GC**TTGGTTAAATGCATC
WTVF	T172V	CTTGGTATCACAGCC**GT**TCCAATATTTTCATCAAGC
WTVR	T172V	GCTTGATGAAAAATATTGGA**AC**GGCTGTGATACCAAG

Site-Directed Mutagenesis Kit (Stratagene, La Jolla, CA). For α-DsbA1CA, both cysteine residues of the second disulfide were changed to alanine (C97A and C146A). For α-DsbA1TV, the mutation T172V was made to the residue preceding the *cis*Pro. Primers used are listed in Table 2. The presence of desired mutations was confirmed by DNA sequencing. Constructs were transformed into BL21(DE3)pLysS for overexpression purposes (35). For crystallization, proteins were oxidized with 1.7 m*M* copper(II)(1,10-phenanthroline)$_3$ (Cu(II)Phen$_3$) (34) and concentrated to 11 mg/ml. Selenomethionine (SeMet) α-DsbA1 was prepared by using methods described previously (34).

Redox parameters

The pK_a value of the nucleophilic active site cysteine was determined by a thiolate-specific increase in absorbance at 240 nm after formation of the thiolate anion (45). Measurements were carried out at room temperature (RT) in 10 m*M* Tris, 10 m*M* sodium citrate, 10 m*M* K_2HPO_4, 10 m*M* KH_2PO_4, 200 m*M* KCl, and 1 m*M* EDTA, adjusted with NaOH or HCl to the respective pH. Reduced protein was prepared by incubating the sample with 10 m*M* DTT at RT for 30 min, and oxidized protein was prepared with Cu(II)-Phen$_3$. Reducing or oxidizing agents were removed by using a PD10 column (GE Healthcare, Piscataway, NJ). The initial assay volume was 2 ml and contained 20 μM protein. Absorbance of the samples was measured at 240 and 280 nm as the pH was reduced in steps of 0.2 pH units by using 0.2 *M* HCl. EcDsbA or EcDsbC was used as a control. For statistical purposes, three samples were measured in parallel and data averaged. The entire experiment was repeated at least twice for each protein.

The pH-dependent specific absorbance of the thiolate anion was measured and corrected for volume increase and buffer absorbance ($[A_{240}/A_{280}]_{red}/[A_{240}/A_{280}]_{oxid}$). The p$K_a$ value was calculated by fitting the data to the Henderson-Hasselbalch equation:

$$\mathrm{pH} = \mathrm{p}K_a - \log\left([A_{240}/A_{280}]_{red}/[A_{240}/A_{280}]_{oxid}\right)$$

Measurement of the redox potential of α-DsbA1 and variants was performed in the presence of different ratios of oxidized (GSSG) and reduced (GSH) glutathione (0–10 m*M* total glutathione). Protein samples (1 μM) were incubated for 24 h at RT in 100 m*M* phosphoric acid/NaOH, 1 m*M* EDTA pH 7 and different ratios of GSH/GSSG. The change in fluorescence intensity by using an excitation wavelength 280 nm was measured at the maximum emission wavelength (330 nm) by using a fluorescence spectrophotometer (Photon Technology International, Seefeld, Germany).

Redox potentials were calculated by using the Nernst equation and the glutathione standard potential ($E^{0'}_{GSH/GSSG} = -240$ mV):

$$E^{0'} = E^{0'}_{GSH/GSSG} - (RT/nF)\ \ln K_{eq},$$

where RT is the product of the gas constant and the absolute temperature, n is the number of electrons transferred, and *F* is the Faraday constant. The equilibrium constant K_{eq} was estimated according to the equation:

$$Y_{obs} = [Y_{ox} + (M/K_{eq}) \times Y_{red}]/[1 + (M/K_{eq})]$$

where Y_{obs} is the fraction of reduced protein at equilibrium, Y_{ox} and Y_{red} are the signals for the oxidized and reduced proteins, respectively, and M is the ratio of $[GSH]^2$ to [GSSG].

Biochemical assays

We used an *in vitro* ubiquinone reduction assay to determine whether α-DsbA1 and variants were substrates of EcDsbB. Reduced protein (15 μM) in 50 m*M* Na phosphate, 300 m*M* NaCl, and 0.1% (wt/vol) *N*-dodecyl-maltoside at pH 6 was added to 15 μM ubiquinone 1 (Q1) (Sigma-Aldrich, Castle Hill, NSW, Australia) in the same buffer, and the reaction was started with the addition of 0.1 μM reduced EcDsbB (3). The reduction of Q1 was followed *via* the absorbance change at 275 nm. EcDsbA was used as a positive control. *In vitro* disulfide reductase activity of α-DsbA1 was measured by the ability of the protein to catalyze the reduction of insulin by DTT, as described previously (26). The reaction mixtures were freshly prepared in 1-ml cuvettes by adding final concentrations of 0.13 m*M* insulin (Sigma), 0.33 m*M* DTT, 0.1 *M* sodium phosphate, pH 7, and 2 m*M* EDTA to various concentrations of the catalyst (4–10 μM). The reduction of insulin was monitored by measuring the optical density of the samples at 650 nm for 80 min at 30-s intervals.

The ability of the protein to isomerize disulfide bonds was evaluated by using the scrambled-RNaseA (ScRNaseA) assay. Disulfide-scrambled RNaseA was produced as follows. Native RNaseA (Sigma) was incubated overnight at room temperature in 50 m*M* Tris-HCl, pH 8, in the presence of 6 *M* GdmCl and 150 m*M* DTT. The reduced, unfolded protein was acidified with 100 m*M* acetic acid/NaOH, pH 4, and purified over a PD10 column. The RNaseA concentration was determined spectrophotometrically, and the eight free thiol groups were verified by using Ellman's assay. To generate RNaseA with randomly oxidized disulfides (scRNaseA), reduced RNaseA was diluted to a final concentration of 0.5 mg/ml in 50 m*M* Tris-HCl, pH 8.5, and 6 *M* GdmCl and incubated in the

dark at room temperature for at least 3 days. The randomly reoxidized RNaseA was concentrated, acidified, and purified, as described earlier, and oxidation of disulfide bonds was confirmed by using Ellman's assay. Isomerase activity of test proteins was evaluated by measuring spectrophotometrically the renaturation of scRNaseA. Reactivated RNaseA with native disulfide bridges can cleave cyclic-2′,3′-cytidinemonophosphate (cCMP) into 3′-cytidinemonophosphate (3′CMP), resulting in an increase in absorption at 296 nm. Purified α-DsbA1 or variants (10 μM) were added to 100 mM sodium phosphate, 1 mM EDTA, and 10 μM DTT, pH 7, and preincubated for 5 min at 25°C. To start the assay, 40 μM scRNaseA was added. At several time points, 200 μl aliquots were taken and added to 600 μl of 4 mM cCMP (in 100 mM sodium phosphate, 1 mM EDTA, pH 7), so that the final assay volume was 800 μl. The rate of RNaseA cleavage in the removed aliquots was then monitored spectrophotometrically at 296 nm for 2.5 min, and the fraction of native RNaseA (percentage) was plotted against the incubation time.

Thermal denaturation of α-DsbA1 and variants was determined as described previously (25). Thermal unfolding was monitored at 220.5 nm on a Jasco J-810 spectropolarimeter: 10 μM samples in sodium phosphate buffer, pH 7, were heated from 25°C to 95°C at a constant rate of 1°C/min. Data were normalized by correcting for pre- and posttransitional baselines, and the thermal transition was tentatively fitted according to a two-state model.

EcDsbA complementation

To determine whether α-DsbA1 and the two variants could complement EcDsbA, we cloned the *α-dsbA1* gene and variants, including the *Wolbachia* signal sequence, into the arabinose-inducible pBAD33 vector (20). The constructs were chemically transformed into the nonmotile *E. coli dsbA*$^-$ mutant (JCB817) and plated on LB chloramphenicol plates. Additionally, we tested the ability of wt and variant α-DsbA1s to complement EcDsbA in the absence of EcDsbB, by chemically transforming the *E. coli dsbA*$^-$/*dsbB*$^-$ double mutant (JCB818). To exclude the possibility that complementation of EcDsbA was impaired by failure to export wt or variant α-DsbA1s, constructs also were prepared in which an *E. coli* DsbA signal sequence replaced the *Wolbachia* signal sequence. As a positive control, we used JCB817 and 818 cells harboring pBAD33::EcDsbA. Triplicates of fresh colonies were transferred to minimal agar (M63) containing 40 μg/ml of each amino acid (except tryptophan, which was at 20 μg/ml); arabinose was included at 1 mg/ml to induce expression. Additionally, the experiment was performed by using agar without arabinose to monitor background complementation. The experiment also was performed in the absence and presence of L-cystine to see whether it could act as a general oxidant for α-DsbA1. Plates were incubated for 7–10 h at 37°C before analysis of the diameter of the bacterial lawns.

Structure determination

Crystals of α-DsbA1 and SeMet α-DsbA1 were prepared as described previously (34). Isomorphous crystals of the two variants were obtained by using similar conditions, after 2 days in 22% PEG 3350, 0.1 M ammonium citrate, pH 5.5–5.9. The structure of wt α-DsbA1 was solved with MAD phasing. Native and MAD data were measured at beamline 8.3.1 of the Advanced Light Source (Berkeley, CA). For the two variants, diffraction data were measured by using a high-brilliance FR-E X-ray generator and an R-AXIS IV^{++} imaging plate detector. All crystals were soaked for ~5 min in a cryoprotectant comprising the crystallization solution plus 20% PEG 400.

Data for the wt and SeMet proteins were processed by using HKL2000 (46). SeMet positions were located by using SOLVE/RESOLVE (51), and the phased electron-density map was used for automatic model building with ARP/WARP (44). Manual model building was performed by using COOT (13), and the structure was refined first with CNS (8) and then with PHENIX, including TLS refinement (1). The structure of wt α-DsbA1 includes residues 20 to 218 of the mature 218 residue protein, with one molecule in the asymmetric unit. No density was observed for the N-terminal 19 residues or the octa-His affinity tag. Where appropriate, residues were modelled with alternate conformations, and side chains of residues with weak density were modelled with reduced occupancy. For α-DsbA1TV and α-DsbA1CA, diffraction data were processed with CrystalClear 1.3 (Rigaku Americas, Houston TX), and the structures were solved with difference Fourier methods from the native α-DsbA1 structure. The final structures include residues 20 to 218 for α-DsbA1TV and 19 to 218 for α-DsbA1CA. Two PEG molecules are bound in the wt and CA variant structures; one at the active site, and one in a groove on the helical domain. In the TV mutant, the active-site PEG is present, but evidence for the second PEG is less convincing, and this region is instead modelled as a series of waters.

MolProbity (11) was used to assess the quality of the crystal structures. SSM (33) was used to compare α-DsbA1 with other TRX-fold structures. Structural figures were generated by using PyMOL (Warren L. DeLano, The PyMOL Molecular Graphics System, http://www.pymol.org) and APBS (4). Torsional energies of disulfides were estimated by interpolation of a potential-energy surface calculated for diethyl disulfide around its three critical dihedral angles corresponding to disulfide dihedral angles χ^2, χ^3, and $\chi^{2'}$ at 10-degree increments. Quantum chemical calculations were performed at the MP2 level of theory (21). Contributions of χ^1 and $\chi^{1'}$ were estimated by using terms from a torsional potential-energy function from AMBER (47).

The coordinates and structure factors for wt and TV and CA variants of α-DsbA1 structures have been submitted to the PDB with accession codes 3F4R, 3F4S, and 3F4T, respectively.

Results

α-DsbA1 is less oxidizing than EcDsbA

Previously, we showed that α-DsbA1 is an oxidoreductase on the basis of its activity in two standard assays for thiol-disulfide oxidoreductase activity (35). Here we characterized α-DsbA1 further and found that its redox properties are different from those of EcDsbA (Table 3). First, it is less oxidizing than EcDsbA (its redox potential is −163 mV compared with −122 mV for EcDsbA), and the pK_a of its nucleophilic cysteine (presumed to be Cys51 on the basis of sequence and structure conservation with all other TRX-fold proteins) is more than one pH unit higher than that of EcDsbA (~5 compared with ~3.3) (Table 3). Further, α-DsbA1—unlike EcDsbA—has a second disulfide bond, although this appears to have little influence on the redox properties of the enzyme (see our analysis of the α-DsbA1 CA variant later).

Table 3. Summary of α-DsbA1 Redox Parameters

	pK_a[a]	K_{eq} (M)[b]	$E^{o'}$ (mV)[b]	*Insulin reduction*[c]	*scRNase assay*[d]	*EcDsbB interaction*[e]
wt α-DsbA1	4.65 ± 0.08	$2.2 \pm 0.27 \times 10^{-3}$	−163	29%	58%	0
α-DsbA1TV	4.69 ± 0.08	$4.1 \pm 0.34 \times 10^{-3}$	−170	40%	38%	0
α-DsbA1CA	5.00 ± 0.06	$2.0 \pm 0.17 \times 10^{-3}$	−161	29%	54%	0
EcDsbA	3.28 ± 0.09	$1.2 \pm 0.05 \times 10^{-4}$	−122	31%	40%	100%
EcDsbC	4.1 ± 0.3	$1.95 \pm 0.06 \times 10^{-4}$	−130	100%	92%	0
SaDsbA	3.37 ± 0.07	$2.09 \pm 0.27 \times 10^{-4}$	−131	0	22%	0

[a]See Fig. 2A; value for EcDsbA from (28); value for EcDsbC from (50); value for SaDsbA from (25).
[b]See Fig. 2B; value for EcDsbA from (28); value for EcDsbC from (60); value for SaDsbA from (12).
[c]See Fig. 2C; value for SaDsbA from (25). Activity of EcDsbC taken to be 100%.
[d]See Fig. 2D; value for EcDsbA from (35); value for SaDsbA from (25). Activity of folded RNase A taken to be 100%.
[e]See Fig. 2E; value for EcDsbC from (3); value for SaDsbA from (25). Activity of EcDsbA taken to be 100%.

α-DsbA1 does not complement EcDsbA deficiency and is not a substrate of EcDsbB

We evaluated whether α-DsbA1 catalyzes disulfide formation in *Escherichia coli in vivo* by determining whether it complements EcDsbA in *dsbA*- and *dsbA/dsbB*-null backgrounds. EcDsbA is not essential for cell viability, but its deletion in *E. coli* leads to pleiotropic phenotypes. One such phenotype is the loss of functional flagellae, resulting in loss of motility on soft agar plates. We found that α-DsbA1 did not complement either *dsbA*- or *dsbA/dsbB*-null strains (Fig. 1). Further, we found that unlike EcDsbA, α-DsbA1 is not a substrate of EcDsbB (Table 3, Fig. 2E).

α-DsbA1 has a DsbA-like architecture

We solved the crystal structure of α-DsbA1 by MAD methods and refined it to a resolution of 1.6 Å, with R-factor and R-free values of 16.5% and 19.3%, respectively (Fig. 3, Table 4). The α-DsbA1 structure comprises two domains, a TRX-fold (residues 20 to 82 and 163 to 218) and an inserted helical domain (residues 83 to 162), so that the architecture is broadly similar to that of EcDsbA (17). However, the topology of α-DsbA1 diverges from that of EcDsbA, in that the N-terminal strands of the two proteins are hydrogen bonded to opposite edges of the central β-sheet (Fig. 3). Further, the structures of α-DsbA1 and EcDsbA do not superimpose well, with an RMSD of 3.1 Å for 143 of the 199 C_α. To some extent, this poor match is a consequence of different relative orientations of the two domains, because matches between the isolated TRX and helical domains of the two proteins are somewhat better (2.4 Å/70 C_α and 1.9 Å/61 C_α, respectively). Nonetheless, α-DsbA1 has features that appear to be unique among structurally characterized DsbAs.

The α-DsbA1 surface is basic and lacks the hydrophobic features of EcDsbA

The characteristic surface features of EcDsbA and DsbAs from *Vibrio cholerae* (TcpG) (27) and *Neisseria meningitidis* (NmDsbA3) (54) include a hydrophobic groove and a hydrophobic patch (Fig. 3) thought to be important for binding unfolded protein substrates (41). The hydrophobic groove of EcDsbA also interacts with a periplasmic loop of its redox partner EcDsbB (29). The surface features of α-DsbA1 differ markedly from these. Most important, the surface is basic rather than hydrophobic: many residues contributing to the hydrophobic patch of EcDsbA are replaced by polar or charged residues in α-DsbA1 (Fig. 3). Moreover, as a consequence of the shorter loop between β5 and α7 in α-DsbA1 compared with EcDsbA, no hydrophobic groove is present on the surface of α-DsbA1 (Fig. 3). The absence of the hydrophobic groove in α-DsbA1 may explain the lack of interaction between α-DsbA1 and EcDsbB in the *in vitro* results described

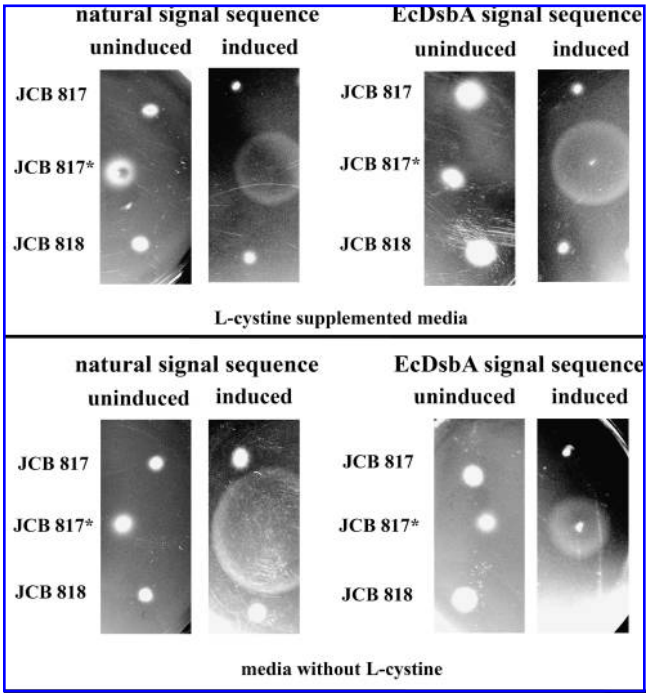

FIG. 1. EcDsbA and EcDsbA/EcDsbB *in vivo* complementation assays. *In vivo* complementation of the motility of an *E. coli* dsbA null mutant (JCB817) and an *E. coli dsbA/dsbB* null mutant (JCB818). Two different constructs of α-DsbA1 were tested. Construct 1 contains the *W. pipientis* signal sequence and construct II the EcDsbA signal sequence prior to *α-dsbA1* (cloned into the pBAD33 vector). Shown are uninduced (no arabinose to monitor background complementation, negative control) and induced plates (containing arabinose). As a positive control, we used JCB817 cells harboring pBAD33::*EcdsbA* (JCB817*). To assess DsbA complementation we evaluated restoration of *E. coli* motility as the presence of a halo of growth around the point at which the cells were stabbed in the agar, as seen in the induced positive control JCB817*. α-DsbA1, and the two variants (not shown), did not complement either strain in any of the conditions tested.

earlier, because this groove is important for the interaction between EcDsbA and EcDsbB (29).

α-DsbA1 structure is more similar to SaDsbA than to EcDsbA

To identify closer structural matches to α-DsbA1 than to EcDsbA, we performed an alignment by secondary structure matching by using SSM (33) against the entire PDB. Only one statistically significant structural similarity (P score >3.0) was identified (Table 5): a conserved protein of unknown function from the gram-positive organism *Enterococcus faecalis* EF3133 (PDB code, 1Z6M). Other matches were 2IMF, a κ-class glutathione *S*-transferase [the structural relation between κ-GSTs and DsbA has been noted previously (14)]; 3BCI, the DsbA from the gram-positive organism *Staphylococcus aureus* (SaDsbA) (25); and 2IN3, a putative "protein disulfide isomerase" from the gram-negative *β*-proteobacterium, *Nitrosomonas europa*. Neither 1Z6M nor 2IN3 has been reported in the literature, but their architecture of a TRX fold with an inserted four-helix domain, and the presence in each of a CXXC motif and a *cis*Pro loop suggest that both are redox active (Table 5). Surprisingly, the highest sequence identity was with a DsbA from a gram-positive organism, SaDsbA: 21% overall and 25% for residues in the TRX fold. However, the redox properties and enzyme activities of α-DsbA1 and SaDsbA are very different (Table 3).

The structural similarity between α-DsbA1 and proteins of the κ-class of GSTs prompted us to investigate whether α-DsbA1 has GST activity, but we were unable to detect GST activity for α-DsbA1, even at very high concentrations (20 μM) of the protein (Fig. 4).

The catalytic disulfide of α-DsbA1 is strained

Redox activity of TRX-fold proteins is mediated by the CXXC active-site motif, located at the N-terminus of helix α1, where the two cysteines can interconvert between dithiol and disulfide forms; α-DsbA1 has the sequence $C_{51}YHC_{54}$. Although α-DsbA1 crystals were grown from oxidized protein, the electron density suggests a mixture of oxidized and reduced forms for the catalytic disulfide, and the structure was modelled as a mixture of both. Reduction of redox-active disulfides commonly occurs as a result of radiation damage (2, 55) and has been observed, for example, in SaDsbA (25) and yeast PDI (53). It is noteworthy that the second disulfide bond of α-DsbA1 remains oxidized in the crystal structure, indicating that it is resistant to reducing conditions and is not redox active.

Conformational analysis of the disulfide of oxidized α-DsbA1 indicates a high torsional energy (19.5 kJ/mol or 4.5 kcal/mol), mainly due to χ^2 of the reactive Cys51 and χ^3, the torsion angle about the disulfide bond between Cys51 and Cys54, which are both two standard deviations from normal. χ^1 of Cys 54 the resolving cysteine is also in an unusual conformation (−46 degrees), one standard deviation from normal. On disulfide reduction, most of this strain is lost, with only χ^1 of Cys51 adopting a slightly strained conformation (−165 degrees) one standard deviation from normal. Similar oxidized and reduced conformations are present in other TRX-fold redox proteins, suggesting that disulfide torsional strain is a common feature of these proteins.

We also investigated interactions that might help stabilize the nucleophilic cysteine of α-DsbA1 and contribute to its low pK_a. We found that the Sγ atom of reduced Cys51 is within hydrogen-bonding distance of the Sγ and main-chain nitrogen of Cys54 (Table 6); similar interactions are observed in other TRX-fold redox proteins (5, 23). In addition, Cys54 Sγ is within hydrogen-bonding distance of the side-chain hydroxyl of Thr172, although we know from our mutation data that this residue contributes little to the reduced pK_a of Cys51 (Table 3, Fig. 2A). The very basic surface surrounding the redox-active site may contribute to a low pK_a for Cys51.

FIG. 2. Characterization of α-DsbA1, α-DsbA1TV, and α-DsbA1CA. (**A**) pK_a determination of the nucleophilic cysteine of α-DsbA1 (○, *grey curve*), α-DsbA1TV [▲, *black curve* (overlays on grey curve)], and α-DsbA1CA (■, *dashed curve*). The pH-dependent specific absorbance signal of the thiolate anion was measured, normalized, and fitted according to the Henderson-Hasselbalch equation. (**B**) Redox equilibria of α-DsbA1 (○), α-DsbA1TV (▲), and α-DsA1CA (■) with glutathione at pH 7 and 25°C. The ratio of reduced α-DsbA1 and variants was measured by using the specific fluorescence intensity of the protein at 330 nm with an excitation wavelength of 280 nm. (**C**) Catalyzed reduction of insulin by DTT. Reduction of insulin (131 μM) was measured in 0.1 *M* sodium phosphate buffer, pH 7, 2 m*M* EDTA. The reaction was performed in the absence (×) or presence of 4 μM EcDsbC (■), 10 μM EcDsbA (●), 10 μM α-DsbA1 (○), 10 μM α-DsbA1TV (□), or 10 μM α-DsbA1CA (△). Reactions were started by adding DTT to a final concentration of 0.35 m*M*, and the aggregation of reduced insulin was followed by the increase in optical density at 650 nm. (**D**) The *in vitro* isomerase activity was assessed by using the scrambled RNaseA (scRNaseA) refolding assay. In brief, scRNaseA enzyme (40 μM) was incubated in 0.1 *M* sodium phosphate buffer, pH 7.0, 1 m*M* EDTA, 10 μM DTT in the absence (*, negative control) or presence of 10 μM DsbC monomer (■), 10 μM αDsbA1 (○), 10 μM α̃DsbA1TV (□), or 10 μM α̃DsbA1CA (△). RNaseA activity was assayed by monitoring cCMP hydrolysis spectrophotometrically at 296 nm. As a positive control, we performed additional reactions with folded RNaseA, which was normalized to 100% RNaseA activity. The fraction of native RNaseA (in percentage) activity were calculated and plotted against incubation time. (**E**) EcDsbB-catalyzed reduction of ubiquinone (Q1) by reduced Dsb proteins. The ability of 15 μM of reduced EcDsbA (●), EcDsbC (×), α-DsbA1 (○), α-DsbA1TV (▲), or α-DsbA1CA (■) to reduce 15 μM Q1 was evaluated. The reaction was initiated by addition of 0.1 μM EcDsbB (arrow) and monitored *via* the decrease in absorbance at 275 nm. EcDsbA was able to reduce Q1 with an initial velocity of 190 m*M* min/mM EcDsbB, whereas α-DsbA1 and variants proved not to be EcDsbB substrates. (**F**) Thermal denaturation data for α-DsbA1CA in 0.1 *M* sodium phosphate buffer, pH 7. Plots are shown for oxidized (■) and reduced (□) α-DsbA1CA. The oxidized redox-active site destabilizes the structure of α-DsbA1CA compared with the reduced form, as evidenced by the shift to the left of the oxidized form. The melting temperature T_m of oxidized α-DsbA1CA is 330.7 ± 0.05 K, and that of reduced α-DsbA1CA is 336.9 ± 0.05 K. Similarly, oxidized EcDsbA is also less stable than reduced EcDsbA (T_m values of 342.4 ± 0.05 and 350.6 ± 0.52 K, respectively) (25).

α-DsbA1 has a flexible cisPro loop

The second conserved feature of redox-active TRX-like proteins is the *cis*Pro loop, which is close in space but distant in sequence from the redox-active CXXC site, and which is involved in substrate interactions (32, 37, 39). A Thr precedes the *cis*Pro residue of isomerases EcDsbC and EcDsbG. The hydrophilic nature of this residue and its proximity to the nucleophilic cysteine is thought to be important for Dsb isomerase activity (5, 23). By comparison, the residue

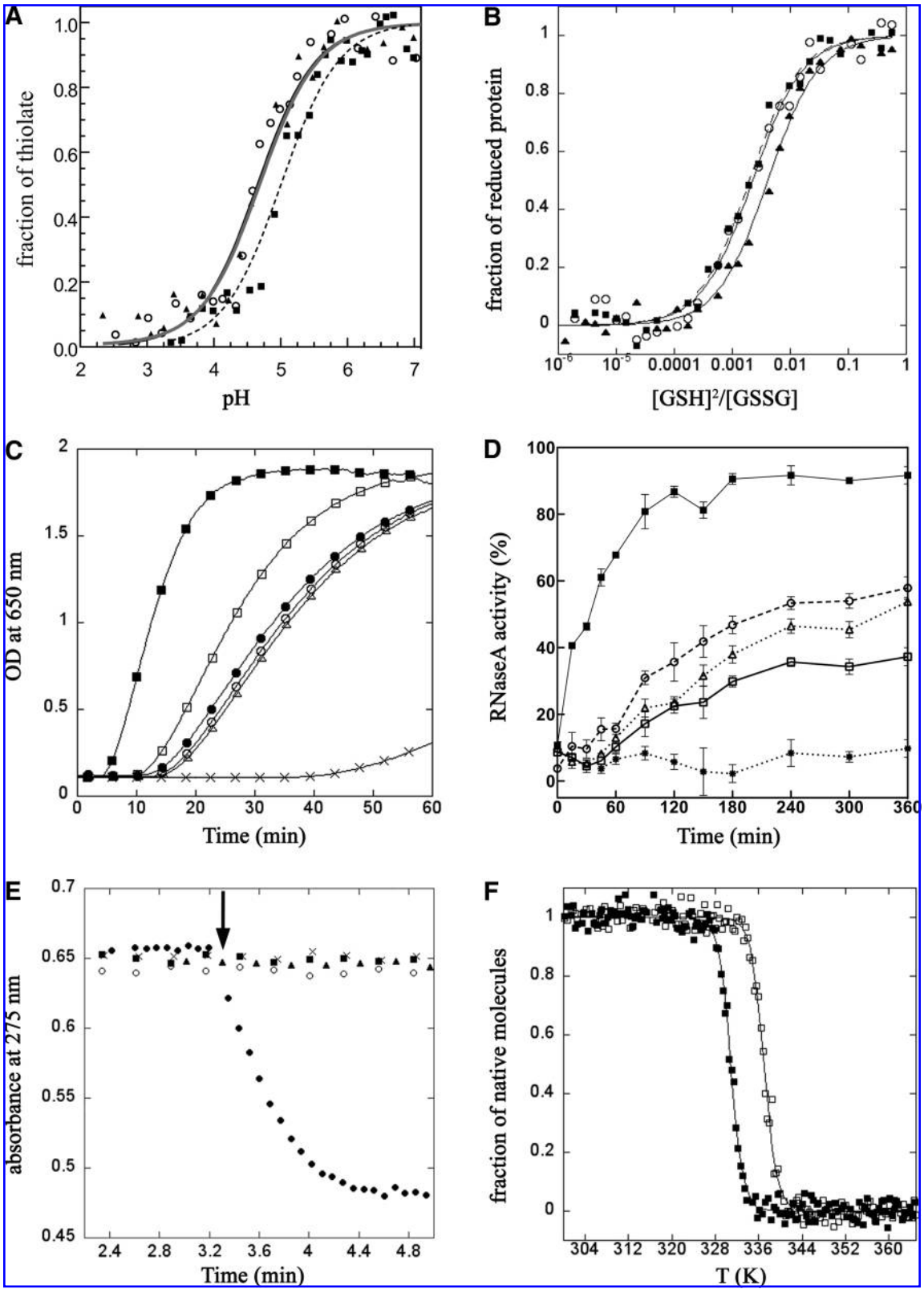

preceding the *cis*Pro in EcDsbA is Val. Our analysis of proteobacterial DsbAs found that Val is highly conserved at this position in γ-proteobacterial DsbAs, like EcDsbA, whereas it is an invariant Thr in α-proteobacterial DsbAs (Table 1).

We anticipated that α-DsbA1 Thr172 would form interactions similar to those observed in the Dsb isomerases. Unexpectedly, we found considerable differences in this region compared with other TRX-fold proteins. First, we observed flexibility in the *cis*Pro loop so that two conformations were modelled for residues 171 through 174 (Fig. 5). Second, the residues T_{172}*cis*P_{173} are translated in space with respect to the CXXC active sites of other TRX-fold proteins, so that Thr172 hydroxyl is closer in space to the second cysteine of the CXXC active site (Cys54) than to the nucleophilic cysteine (Cys51) (Table 6). In other TRX-fold proteins with a Thr at this position (EcDsbC, EcDsbG, SaDsbA), the equivalent Thr is located closer in space to the nucleophilic cysteine (Fig. 5) and contributes to the redox properties (48).

Thr172 modulates redox activity

To investigate whether Thr172 might contribute to redox activity and the observed mobility of the *cis*Pro loop in α-DsbA1, we mutated it to the EcDsbA-like residue Val (α-DsbA1TV). The crystal structure of α-DsbA1TV, determined to 1.55-Å resolution, revealed the *cis*Pro loop to be less mobile than that of the wt protein: a single conformation for residues 171 through 174 was sufficient to fit the electron density (Fig. 5), confirming a role for Thr172 in loop flexibility. The mutated Val172 side chain adopts a different conformation to that of Thr172 in the wt protein: it is more like that of other Dsb structures, rotated away from the active-site cysteines, and closer to the nucleophilic Cys51 (Fig. 5 and Table 6). These structural changes are accompanied by a decrease in the redox potential from −163 to −170 mV in the α-DsbA1TV variant (Table 3). Interestingly, α-DsbA1TV is more active than wt α-DsbA1 in the insulin-reduction assay, but it is a poorer isomerase (Table 3). These results confirm the role of the residue preceding the *cis*Pro in the redox properties and substrate interactions of TRX-fold family of proteins (48). Like the wt protein, α-DsbA1TV does not interact with EcDsbB *in vitro*, it does not complement EcDsbA *in vivo*, and it has no GST activity (Figs. 1, 2E, and 4).

α-DsbA1 has a second disulfide

We predicted on the basis of their conservation in α-DsbA sequences (Table 1), that Cys97 and Cys146 would form a second disulfide bond in α-DsbA1. The crystal structure of α-DsbA1 confirms this prediction, showing that the Cys97-Cys146 disulfide links the C-termini of two helices (α2 and α5) in the helical domain (Figs. 3 and 6). Unlike the active-site disulfide, no evidence exists of x-ray–induced reduction of this disulfide either in wt α-DsbA1 or in α-DsbA1TV structures, suggesting that this disulfide is resistant to reduction. However, analysis of this disulfide indicates that Cys97 adopts a low-probability rotamer conformation. Consequently, the disulfide has a high predicted torsional stress (27 kJ/mol, or 6.3 kcal/mol).

Disulfides that introduce local stress in folded proteins may have functional rather than structural roles (57). To investigate this possibility, we mutated both Cys97 and Cys146 to alanine (α-DsbA1CA) and characterized this variant. Little difference was noted in the overall fold of the variant structure compared with wt α-DsbA1. However, the main-chain oxygen of Ala142 is oriented differently in the wt and α-DsbA1CA variant, presumably because of steric constraints imposed by the disulfide (Fig. 6).

The α-DsbA1CA variant allowed analysis of the effect of the active-site disulfide on the stability of the protein. We found that like EcDsbA, and unlike most protein disulfides, the active-site disulfide of α-DsbA1 is destabilizing (Fig. 2F). The pK_a of the nucleophilic cysteine of α-DsbA1CA is a little higher than that of wt (pK_a, 5.0 and 4.65, respectively), but otherwise, the redox parameters and activities of α-DsbA1CA are similar to those of wt α-DsbA1 (Table 3; Figs. 1, 2, and 4).

Discussion

Strong oxidants like EcDsbA have high redox potentials (−122 mV) and low equilibrium constants for forming

FIG. 3. Structure of α-DsbA1 and comparison with EcDsbA. (A) Ribbon representation of α-DsbA1 and EcDsbA (19, 41). Both α-DsbA1 and EcDsbA have a catalytic TRX domain (green) and an inserted helical domain (blue). The active-site cysteines and the additional cysteine pair of α-DsbA1 are shown as yellow spheres. (**B**) Topology of the TRX folds of α-DsbA1 and EcDsbA. α-Helices are shown as rectangles, and β-strands, as arrows. The architecture of the TRX fold (black) consists of an N-terminal βαβ and a C-terminal ββα motif connected by an α-helix (40). The inserted α-helical domains of α-DsbA1 and EcDsbA (formed from four helices and an extension to helix α6 and comprising 68 and 65 residues, respectively) is indicated by a blue box. Departures from the common TRX-fold are shown in green. The locations of the active-site redox cysteines and the additional cysteine pair of α-DsbA1 are shown by *yellow circles*, and the *cis*Pro loop, by a *red circle*. The topologies of the two proteins diverge at the N-terminus: the N-terminal β-strand (β1) of α-DsbA1 and EcDsbA are positioned at opposite edges of the β-sheet, and α-DsbA1 has a short helix (α0) preceding this strand. (**C**) Electrostatic surfaces of α-DsbA1 and EcDsbA. Red indicates negatively charged (−5 kT) and blue positively charged regions (+5 kT). Uncharged surfaces are shown in white. The PEG molecule bound near the redox-active site of α-DsbA1 is shown (green spheres). The position of the nucleophilic cysteine in both structures is denoted by "S." The second disulfide of α-DsbA1 is on the opposite surface of α-DsbA1 (not shown). The surface of α-DsbA1 is very basic and lacks the characteristic hydrophobic groove and hydrophobic patch surrounding the active site of EcDsbA and other structurally characterized γ-proteobacterial DsbAs. (**D**) Structure-based sequence alignment of α-DsbA1 and EcDsbA. Secondary structure elements of α-DsbA1 are depicted as rectangles for helices and arrows for strands, and are labelled and underlined for EcDsbA. No electron density was observed for the N-terminal α-DsbA1 residues shown in grey. The redox-active site, the *cis*Pro loop, and the second cysteine pair of α-DsbA1 are shown in red. Residues contributing to the hydrophobic surface surrounding the active site of EcDsbA are shown in magenta for the hydrophobic patch and green for the hydrophobic groove. Residues contributing to the basic surface surrounding the active site of α-DsbA1 are shown in blue. (For interpretation of the references to color in this figure legend, the reader is referred to the web version of this article at www.liebertonline.com/ars).

disulfides with glutathione ($K_{eq} = 0.12 \pm 0.05 \times 10^{-3}$ *M*) (15, 28). By contrast, disulfide reductants like EcTRX have low redox potentials [$E^{0'} = -271$ mV/-284 mV (9, 48)] and high equilibrium constants [$K_{eq} = 10$ *M* (38)]. The oxidizing power of EcDsbA is thought to originate from two interrelated factors: an unusually low pK_a of 3.3 for the reactive cysteine Cys30 of EcDsbA (28) compared with the more usual value of ~9 for a cysteine thiol (52), and greater energetic stability of reduced DsbA over the oxidized form (59). In comparison, the pK_a value for the nucleophilic cysteine of EcTRX is ~7, and the active site of EcTRX is in the reduced form at physiologic pH (10).

Here we focused on *Wolbachia pipientis w*Mel DsbA, or α-DsbA1, to our knowledge the first *Wolbachia* protein and the first α-proteobacterial DsbA crystal structure to be reported. We showed that α-DsbA1 differs significantly in its structure and function from EcDsbA. First, although it has similar isomerase and reductant activities to those of EcDsbA in standard assays, α-DsbA1 is much less oxidizing, with a redox potential 40 mV lower and a pK_a value for the nucleophilic cysteine >1 pH unit higher than those for EcDsbA (Table 3). Further, α-DsbA1 has a second disulfide bond, and the cysteines forming the second disulfide are highly conserved in α-DsbA sequences (Table 1). Serendipitously, a PEG molecule

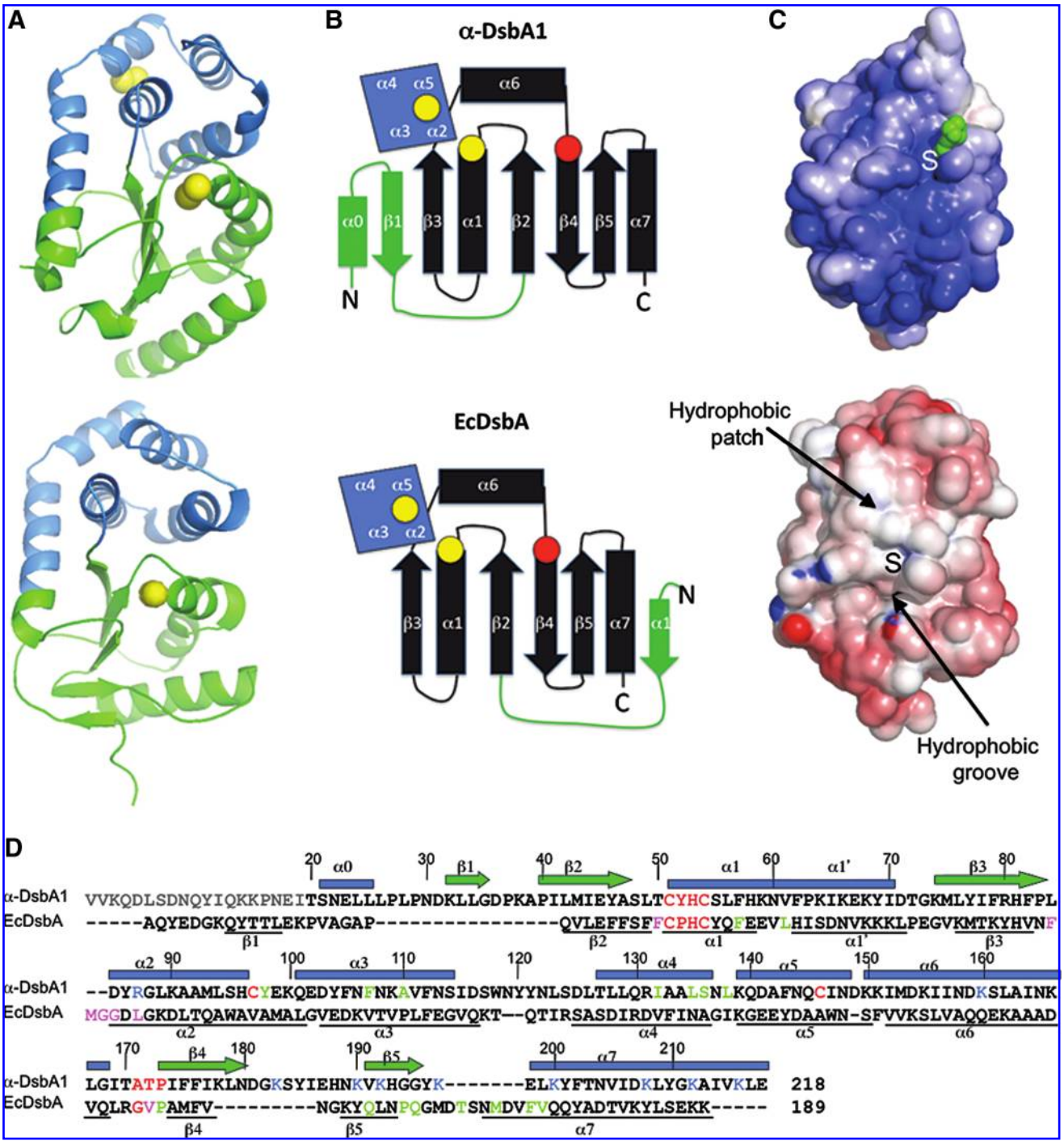

Table 4. X-ray Crystallography Data Collection and Refinement Statistics

		SeMet α-DsbA1 (MAD data)				
Data collection	*Peak*	*Inflection point*	*Remote*	*wt α-DsbA1*	*α-DsbA1TV*	*α-DsbA1CA*
Wavelength (Å)	0.979594	0.979733	0.953725	1.1159	1.5418	1.5418
Resolution range (Å)	50–1.8 (1.86–1.80)	50–1.8 (1.86–1.80)	50–1.8 (1.86–1.80)	50–1.59 (1.66–1.59)	66–1.55 (1.61–1.55)	40–1.85 (1.92–1.85)
Spacegroup	C2	C2	C2	C2	C2	C2
Unit cell: a, b, c, β (Å, Å, Å, °)	71.1, 49.5, 69.7 107	71.1, 49.5, 69.7 107	71.1, 49.5, 69.7 107	71.4, 49.6, 69.7 107	70.7, 49.6, 69.0,106	71.0, 49.5, 69.3, 106
Unique reflections[a]	21,545 (2,125)	21,538 (2,077)	21,596 (2,133)	31,005 (3,039)	31,734	19,850
Redundancy[a]	3.8 (3.7)	3.7 (3.6)	3.8 (3.7)	3.5 (3.0)	2.9 (2.0)	4.1 (3.9)
Completeness[a] (%)	100 (100)	99.7 (97.3)	100 (100)	99.2 (97.4)	94.9 (62.0)	99.9 (99.7)
R_{merge}[a,b]	0.077 (0.207)	0.054 (0.188)	0.049 (0.194)	0.062 (0.277)	0.036 (0.281)	0.056 (0.38)
$\langle V\sigma(I)\rangle$[a]	35.1 (6.9)	35.1 (6.3)	33.1 (5.8)	21.3 (3.0)	15.1 (2.6)	11.7 (2.6)
Refinement statistics	No. reflections ($\|F\| > 0.00$) in working set/test set		27,388/3022 (899/84 for 1.61–1.59 Å)	28,255/3151 (664/86 for 1.57–1.55 Å)		18,601/945 (2,566/117 for 1.95–1.85 Å)
	R_{factor}[c]/R_{free}[d] (%)[a]		16.5/19.3 (18.9/23.4)	15.1/19.4 (21.0/28.4)		17.2/21.0 (21.5/25.7)
Rmsd from ideal	bonds (Å)/angles (°)		0.011/1.3	0.005/0.9		0.006/0.9
Ramachandran plot	favoured/allowed regions (%)		98.4/1.6	99.1/0.8		98.6/1.4
No. of atoms	All/nonsolvent/solvent		2,087/1,821/266	2,023/1,774/249		1,898/1,718/180
Average B factor (Å^2)	All/nonsolvent/solvent		27.2/25.0/41.9	30.0/27.7/45.4		30.9/30.0/39.3
Wilson B			20.8	23.4		26.8

[a]Values in brackets refer to the outermost resolution shell. [b]$R_{merge} = \sum_{hkl}\sum_i |I_i(hkl) - I(hkl)| / \sum_{hkl}\sum_i I_i(hkl)$, where $I_i(hkl)$ is the scaled observed intensity of the ith symmetry-related observation of reflection *hkl* and *I(hkl)* is the average intensity. [c]$R_{factor} = \sum_h |F_o - F_c| / \sum_h |F_o|$, where F_o and F_c are the observed and calculated structure-factor amplitudes for each reflection *h*. [d]R_{free} was calculated for a randomly selected 5% (α-DsbA1CA) or 10% (α-DsbA1 and α-DsbA1TV) of data omitted from refinement.

Table 5. Structural Comparison of αDsbA1 with Other TRX-fold Proteins[a]

	Possible DsbA		*DsbAs*			*Other* E. coli *Dsb proteins*					*κ-class GSTs*	
Protein	X[b]	Y[c]	EcDsbA[d]	VcDsbA[e]	SaDsbA[f]	EcDsbL[g]	EcDsbC[h]	EcDsbG[i]	EcDsbD[j]	EcDsbE[k]	2HCCAI[l]	m-κGST[m]
Function	?Redox	?Redox	Redox	Redox	Redox	Redox	Redox	Redox	Redox	Redox	GST	GST
No. residues	175	204	188	181	165	195	216	229	122	149	203	221
PDB code	1Z6M	2IN3	1FVK:A	1BED	3BCI	3C7M:A	1EEJ:B	1V58:B	2FWG	2B1K	2IMF	1R4W:A
All												
RMSD (Å)	2.0	2.6	3.1	3.1	2.4	3.1	2.8	2.6	2.3	2.9	2.1	3.0
No. C_α	144	152	143	139	130	140	130	128	91	103	146	150
% id	17%	14%	12%	15%	21%	14%	15%	16%	11%	12%	12%	13%
Q-score	0.41	0.33	0.26	0.26	0.31	0.24	0.21	0.20	0.21	0.19	0.36	0.26
P-score	3.9	0.0	0.0	0.0	1.5	0.0	0.9	0.9	1.7	0.0	1.5	0.2
TRX dom												
RMSD (Å)	1.6	2.2	2.4	2.7	1.5	2.8	2.6	2.9	2.2	2.8	2.3	2.2
No. C_α	84	81	70	74	68	68	88	85	74	94	74	67
% id	18%	15%	19%	15%	25%	7%	18%	15%	12%	14%	12%	13%
Q-score	0.27	0.18	0.14	0.14	0.19	0.11	0.18	0.18	0.25	0.27	0.14	0.11
P-score	2.2	0.0	0.0	0.0	0.1	0.0	0.1	0.3	1.2	0.0	0.0	0.0
Helix dom												
RMSD (Å)	2.7 Å	2.1	2.0	1.9	2.2	2.6	2.6	2.8	3.0	3.6	2.0	2.5
No. C_α	68	71	70	61	69	73	40	49	32	36	73	69
% id	10%	13%	6%	16%	17%	11%	18%	10%	6%	6%	8%	9%
Q-score	0.18	0.21	0.23	0.18	0.23	0.19	0.05	0.07	0.05	0.04	0.23	0.16
P-score	0.2	0.6	0.9	0.1	0.3	0.0	0.0	0.0	0.0	0.0	0.6	0.0
WAT1[n]	No	Yes	Yes	Yes	Yes	Yes	Yes	Yes	Yes	Yes	No	No

[a]The SSM server was used to identify structural homologues of α-DsbA1 (7). The PDB files used are representative examples from the results of the SSM search. Matches were sorted by Q-score and P-score. The Q-score uses alignment length and RMSD to assess the match: identical structures have a Q-score of 1. The P-score is the –log of the P value that estimates the probability of achieving the same or a better match by chance. The P-value is a function of RMSD, number of aligned residues, and number of gaps in the alignment. A P-score >3 indicates a statistically significant match (7). The crystal structure of αDsbA1 comprises 199 residues (residues 20 to 218). The TRX domain is formed from residues 20 to 82 and 163 to 218 (119 residues), including the core TRX-fold and additional features (α0, β1). The helical domain comprises residues 83 to 162 (80 residues). The full-length αDsbA1 structure as well as the TRX and helical domains were compared with other structures by using SSM.

[b]Hypothetical protein from *Enterococcus faecalis* V583, unpublished.

[c]Hypothetical protein from *Nitrosomonas europa*, unpublished.

[d]DsbA from *E. coli* (3).

[e]DsbA from *Vibrio cholerae* (TcpG) (6).

[f]DsbA from *S. aureus* (5).

[g]DsbA paralogue with a specific role in uropathogenic *E. coli* (2).

[h]DsbC from *E. coli* (9).

[i]DsbG from *E. coli* (4).

[j]DsbD from *E. coli* (11).

[k]DsbE from *E. coli* (10).

[l]2-Hydroxychromene-2-carboxylate isomerase, a κ class glutathione-S-transferase (GST) from *Pseudomonas putida (13).*

[m]Rat mitochondrial κ-GST (8).

[n]WAT1 is located at the active site of many TRX-fold proteins, although it is sometimes replaced by a bound substrate or ligand (*e.g.,* αDsbA1:PEG, 2HCCA-I:GSH, rGSTK1-1:GSH) or is absent because of crystal contacts (PDB 1Z6M).

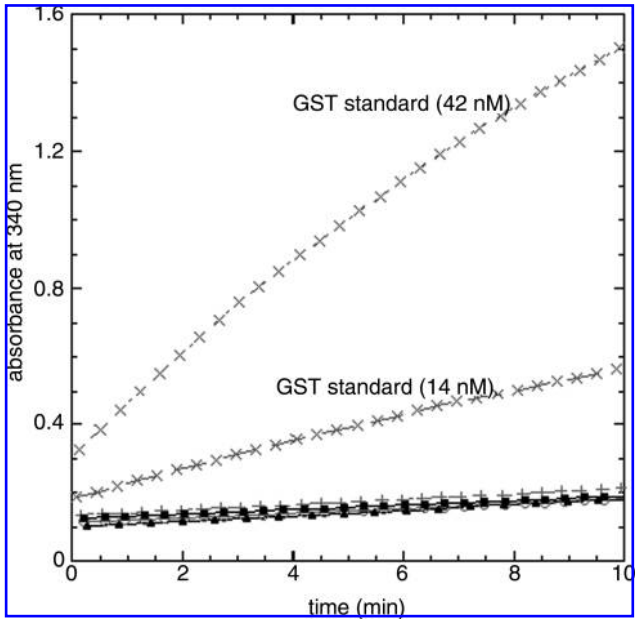

FIG. 4. GST-activity assay. GST activity of α-DsbA1 (○), α-DsbA1TV (▲) or α-DsbA1CA (■) was measured using the GST-tag assay kit (Novagen). Activity was determined by measuring the change in absorbance (A_{340}) specific to the product GSH-CDNB. As a positive control supplied GST (grey ×) was used at two concentrations (14 and 42 nM). Dsb proteins were prepared at a concentration of 20 μM. BSA (20 μM) (+) was used as a negative control. α-DsbA1 and variants do not have GST activity in this assay.

was observed bound near the second disulfide in a groove resembling a peptide-binding site (Fig. 6). The high conservation and unusual conformation of the second disulfide suggested that it might play a regulatory role. However, the α-DsbA1CA variant had redox properties similar to those of wt α-DsbA1. It is, therefore, not possible to determine from these data what function the second disulfide might have.

Surprisingly, the *cis*Pro loop of wt α-DsbA1 was found to be flexible, a feature not previously observed in TRX-fold proteins. This feature is probably a consequence of an unusual interaction between the active-site cysteines and Thr172, the residue preceding the conserved *cis*Pro. Mutation of Thr172 removes the interaction and decreases loop flexibility, supporting the notion that this residue contributes to flexibility in this region. The T172V variant is a more-active reductase than the wt enzyme but a less-active isomerase. These results are in agreement with other work showing that the residue preceding the *cis*Pro contributes to the redox activities and substrate interactions of TRX-fold proteins (48). A Thr preceding the *cis*Pro is a common feature of disulfide isomerases like DsbC/G (23), and a Val in the same position is a common feature of oxidases like DsbA. We wondered whether a Thr at this position of α-DsbA1 might contribute to isomerase properties. We found that this residue does contribute to isomerase activity: mutation from Thr to Val decreases the isomerase activity of α-DsbA1.

We speculate that α-DsbA1 plays a specific role, interacting with a subset of secreted proteins. The fact that the surface surrounding the active site of α-DsbA1 is basic, unlike the hydrophobic surfaces of EcDsbA (18), NmDsbA3 (54) and TcpG (27), lends circumstantial evidence to this notion: α-DsbA1 is unlikely to interact with diverse unfolded protein substrates. Further, the lack of a hydrophobic groove explains why α-DsbA1, unlike EcDsbA (29) and NmDsbA3 (54), does not interact with EcDsbB. Indeed, its structural similarity to SaDsbA suggests that α-DsbA1, like SaDsbA (12, 25) may not require DsbB for activity.

Previously, we identified two waters, WAT1 and WAT2, located at the redox-active site of EcDsbA (19). WAT1 appears to be a conserved feature of many redox-active TRX-fold proteins; it is present in most high-resolution TRX-fold structures that we investigated (Table 5), except those in which ligands were bound or crystal contacts formed at the active site. The conservation of WAT1 in TRX-fold proteins of diverse function, from a range of organisms, and in both redox states, suggests that it plays a role in catalysis, perhaps

TABLE 6. INTERACTIONS OF THE CYS51 THIOL AND THE THR172 HYDROXYL IN THE ACTIVE SITE OF α-DSBA1, COMPARED WITH THE INTERACTIONS OF EQUIVALENT RESIDUES IN OTHER DSBA PROTEINS

	Cys51[a] *Sγ*				*Thr172*[a] *Oγ*[b]	
					Sγ	
Distance (Å) between and	*N His52*	*N Cy53*	*Sγ Cys53*	*PEG/Wat1*	*Cys51*	*Cys54*
wt α-DsbA1[c]	3.9	3.6	3.2	3.2	4.0–4.1	3.1–3.3
α-DsbA1TV[c]	4.0	3.7	3.2	3.2	3.7–4.4	3.8–4.6
α-DsbA1CA[c]	4.1	3.9	3.4	3.3	3.9	3.4
EcDsbA[d]	3.4–3.5	3.3–3.6	3.4–3.5	3.7	4.5–4.6	3.8
EcDsbC[e]	3.8	3.5	3.2	3.5	3.2	3.8
EcDsbG[f]	3.9	3.5–3.7	3.3–3.5	3.3–3.4	3.3–3.4	4.1–4.3
SaDsbA[g]	3.7	3.5	3.2	3.3	4.4[h]	4.6

[a]Or equivalent residue in EcDsbA, EcDsbC, EcDsbG, or SaDsbA.
[b]Or equivalent atom of Val for α-DsbA1TV or EcDsbA.
[c]Distances for reduced form. Ranges are given where two conformations are modelled for Thr172 or Val172.
[d]Distances for reduced EcDsbA (1A2L): WAT1 is not modelled in this structure because of lower resolution so WAT1 distance is from oxidized DsbA (1FVK), and the distance is therefore longer than that for the other structures.
[e]Distances measured from reduced EcDsbC (1TJD).
[f]Distances measured from reduced EcDsbG (1V58).
[g]Distances measured from reduced SaDsbA (1BCI). Interaction is indirect, *via* a water molecule.

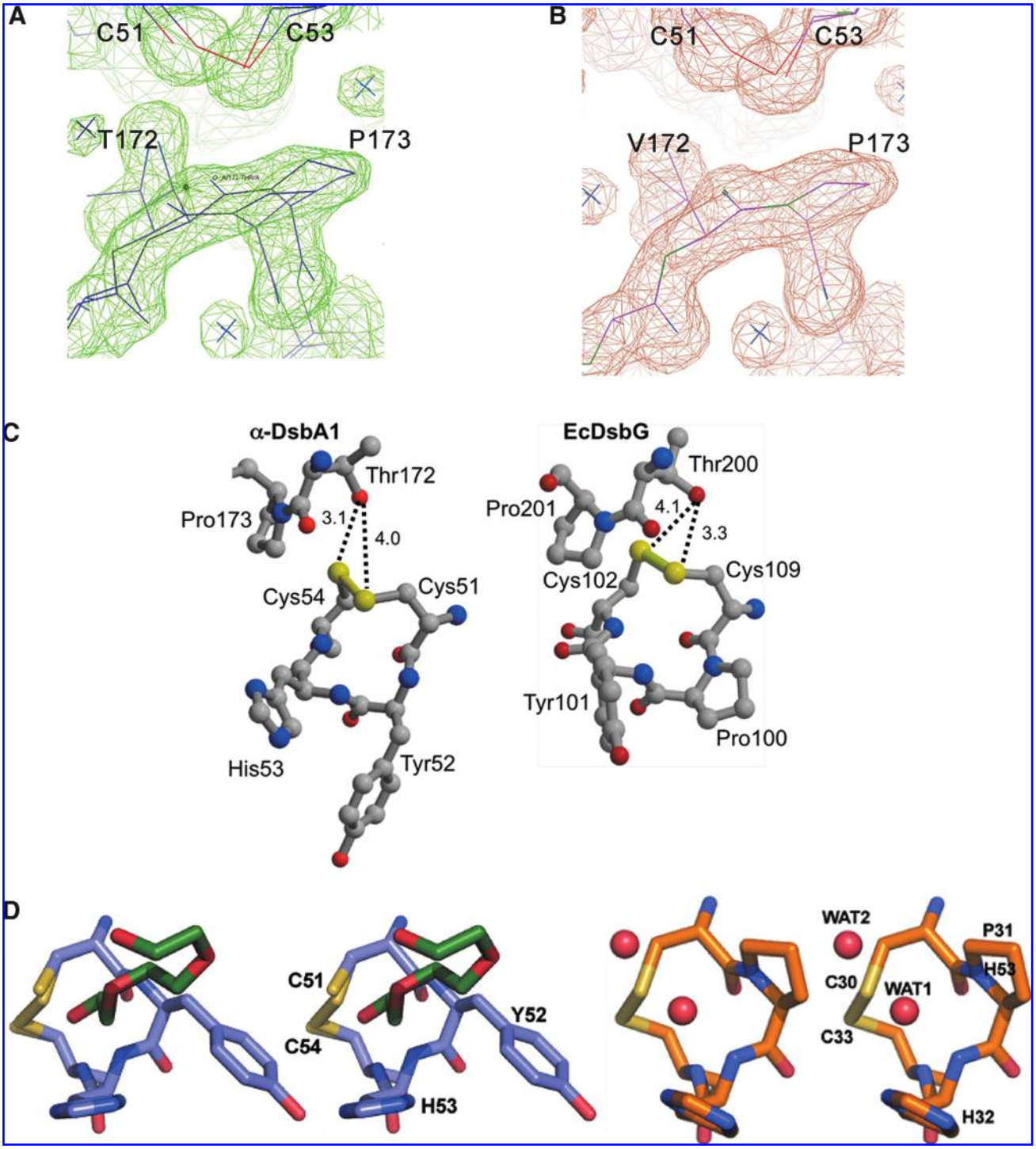

FIG. 5. The redox-active site of α-DsbA1. Electron density ($2F_o$-F_c, contoured at 1σ) at the active site of (**A**) wt α-DsbA1 and (**B**) α-DsbA1TV. The redox-active site is modelled as a mixture of reduced and oxidized cysteines in both structures. The *cis*Pro loop is modelled in two alternate conformations for the wt structure, and a single conformation for α-DsbA1TV, although the side chain of α-DsbA1TV Val172 adopts two conformations in α-DsbA1TV. (**C**) The redox-active site of (*left*) α-DsbA1 and (*right*) EcDsbG (1V58), showing the different interactions formed by the equivalent Thr side chains preceding the *cis*Pro. (**D**) Stereo view of the active-site structures of α-DsbA1 (*left*, blue) and EcDsbA (*right*, orange). The N-terminal hydroxyl of a PEG molecule (green C atoms) in the active site of α-DsbA1 is within hydrogen-bonding distance of Cys51. In EcDsbA, a water molecule (WAT1) is found at the equivalent position (19). WAT1 is conserved in many redox-active TRX-fold proteins (Table 5). (For interpretation of the references to color in this figure legend, the reader is referred to the web version of this article at www.liebertonline.com/ars).

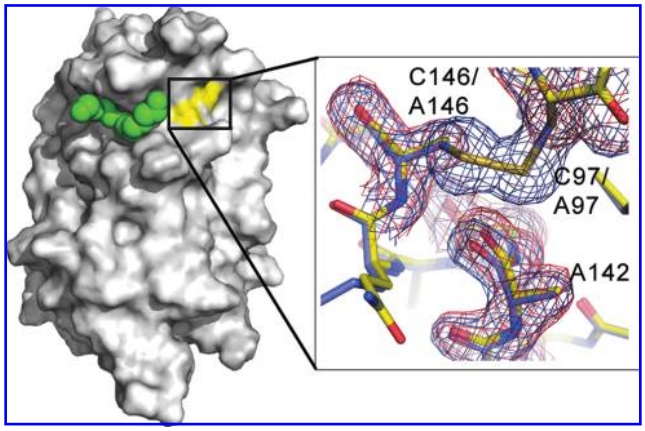

FIG. 6. The second disulfide of α-DsbA1. The additional disulfide of α-DsbA1 (yellow) is located on the protein surface opposite that of the redox-active site disulfide. A PEG molecule (green) is bound near the second disulfide in a groove suggestive of a binding site. The close-up of the region shows superimposed electron-density maps ($2F_o$-F_c contours at 1σ) of wt α-DsbA1 (blue map, blue atoms) and α-DsbA1CA (red map, yellow atoms). The two cysteines (Cys97 and Cys146) are mutated to Ala in α-DsbA1CA: the maps confirm the mutation and also reveal a movement in the backbone oxygen of Ala142. (For interpretation of the references to color in this figure legend, the reader is referred to the web version of this article at www.liebertonline.com/ars).

acting as a general base. Conversely, the structures of ligand-bound complexes, including α-DsbA1 with PEG bound near the active site, show that WAT1 is probably displaced by incoming substrates (Fig. 5). The observed binding interactions of the two PEG molecules in this crystal structure may also provide a starting point for the design of inhibitors for chemical genetics studies. This would facilitate a novel means of investigating the role of α-DsbA1 in inducing *Wolbachia* phenotypes, which cannot be done currently because of the inability to transform the organism.

Taken together, our data show that although α-DsbA1 adopts the DsbA fold associated with oxidase activity, its redox properties suggest that it is a reductase/isomerase. Moreover, the basic residues surrounding the redox-active site and the lack of a hydrophobic groove nearby indicate that α-DsbA1 plays a specialized role in *Wolbachia* biology and that it probably has a narrow, perhaps dedicated, substrate specificity. *E. coli* DsbL also has basic residues surrounding the active site and plays a specific oxidative folding role in uropathogenic *E. coli*. However, the DsbL redox potential is very oxidizing (−95 mV) compared with α-DsbA1, suggesting that they have different redox functions (16). It is possible that α-DsbA1 might play a very different role from that of EcDsbA and other DsbAs that catalyze oxidative folding of secreted proteins; for example, its low redox potential could give rise to antioxidant properties. We know that *Wolbachia* induces the expression of host antioxidant proteins in *Aedes albopictus* cell lines (6) as a protective mechanism. α-DsbA1 could conceivably play a role in defending *Wolbachia* against oxidative stress. Members of the Dsb family are induced together with antioxidant enzymes in the presence of peroxide in the cyanobacterium *Synechocystis* (36). We also point out that *Wolbachia* can only survive as obligate intracellular symbionts inside a vacuole of host origin, suggesting that secreted proteins are exported to the vacuolar compartment where the bacteria reside. Whether or not α-DsbA1 plays a role in oxidative folding of secreted proteins, the mechanisms involved in transferring proteins from the vacuole to the host cytoplasm and *vice versa* are as yet unknown.

Given the important role that redox-active Dsb proteins play in secretion of virulence factors in other organisms (24), the identification of substrate(s) of α-DsbA1, and those of α-DsbA2, and the development of inhibitors that target α-DsbA1 in chemical genetics experiments could help unravel the role of this protein and explain the molecular basis of reproductive host phenotypes induced by this uniquely adapted organism.

Acknowledgments

We are grateful to Prof. James Bardwell (University of Michigan, Ann Arbor, MI) for the gift of vector pBAD33 and bacterial strains. We thank Profs. Tom Alber and Nat Echolls (University of California, Berkeley, CA) for measuring native and MAD data at the Advanced Light Source, which is supported by the Director, Office of Science, Office of Basic Energy Sciences, of the U.S. Dept. of Energy under contract DE-AC02-05CH11231. We thank Karl Byriel for assistance with data collection at the University of Queensland (UQ) ROCX Diffraction facility, and Naomi Haworth (Victor Chang Cardiac Research Institute) for initial energy calculations. This work was supported by the NHMRC (Senior Research Fellowship to J.L.M.), the ARC (project grants to J.L.M., to B.H., and to S.N. and I.I.), UQ (Early Career Researcher Grant to B.H., Postdoctoral Fellowship to S.R.S.), the ETH Zürich and the Schweizer Nationalfond in the framework of the NCCR Structural Biology program (to R.G. and P.F.), and an International Postgraduate Research Scholarship (to M.K.).

Abbreviations

Dsb, disulfide bond; MAD, multiwavelength anomalous diffraction; SeMet, selenomethionine; EcDsbA (B, C, G, D), *E. coli* DsbA (B, C, G, D); TRX, thioredoxin; GSH, reduced glutathione; GSSG, oxidized glutathione; Q1, ubiquinone-1; RNaseA, ribonuclease A; RMSD, root mean square difference; PEG, polyethylene glycol.

Author Disclosure Statement

No competing financial interests exist.

References

1. Adams P, Grosse-Kunstleve R, Hung L, Ioerger T, McCoy A, Moriarty N, Read R, Sacchettini J, Sauter N, and Terwilliger T. PHENIX: building new software for automated crystallographic structure determination. *Acta Crystallogr D Biol Crystallogr* 58: 1948–1954, 2002.
2. Alphey MS, Gabrielsen M, Micossi E, Leonard GA, McSweeney SM, Ravelli RB, Tetaud E, Fairlamb AH, Bond CS, and Hunter WN. Tryparedoxins from *Crithidia fasciculata* and *Trypanosoma brucei*: photoreduction of the redox disulfide using synchrotron radiation and evidence for a conformational switch implicated in function. *J Biol Chem* 278: 25919–25925, 2003.

3. Bader MW, Xie T, Yu CA, and Bardwell JC. Disulfide bonds are generated by quinone reduction. *J Biol Chem* 275: 26082–26088, 2000.
4. Baker NA, Sept D, Joseph S, Holst MJ, and McCammon JA. Electrostatics of nanosystems: application to microtubules and the ribosome. *Proc Natl Acad Sci U S A* 98: 10037–10041, 2001.
5. Banaszak K, Mechin I, Frost G, and Rypniewski W. Structure of the reduced disulfide-bond isomerase DsbC from *Escherichia coli*. *Acta Crystallogr D Biol Crystallogr* 60: 1747–1752, 2004.
6. Brennan LJ, Keddie BA, Braig HR, and Harris HL. The endosymbiont *Wolbachia pipientis* induces the expression of host antioxidant proteins in an *Aedes albopictus* cell line. *PLoS ONE* 3: e2083, 2008.
7. Brownstein JS, Hett E, and O'Neill SL. The potential of virulent *Wolbachia* to modulate disease transmission by insects. *J Invertebr Pathol* 84: 24–29, 2003.
8. Brunger AT, Adams PD, Clore GM, DeLano WL, Gros P, Grosse-Kunstleve RW, Jiang JS, Kuszewski J, Nilges M, Pannu NS, Read RJ, Rice LM, Simonson T, and Warren GL. Crystallography and NMR system: a new software suite for macromolecular structure determination. *Acta Crystallogr D Biol Crystallogr* 54: 905–921, 1998.
9. Cheng Z, Arscott LD, Ballou DP, and Williams CH Jr. The relationship of the redox potentials of thioredoxin and thioredoxin reductase from *Drosophila melanogaster* to the enzymatic mechanism: reduced thioredoxin is the reductant of glutathione in *Drosophila*. *Biochemistry* 46: 7875–7885, 2007.
10. Chivers PT and Raines RT. General acid/base catalysis in the active site of *Escherichia coli* thioredoxin. *Biochemistry* 36: 15810–15816, 1997.
11. Davis IW, Leaver-Fay A, Chen VB, Block JN, Kapral GJ, Wang X, Murray LW, Arendall WB, Snoeyink J, Richardson JS, and Richardson DC. MolProbity: all-atom contacts and structure validation for proteins and nucleic acids. *Nucleic Acids Res* 35: W375–W383, 2007.
12. Dumoulin A, Grauschopf U, Bischoff M, Thony-Meyer L, and Berger-Bachi B. *Staphylococcus aureus* DsbA is a membrane-bound lipoprotein with thiol-disulfide oxidoreductase activity. *Arch Microbiol* 184: 117–128, 2005.
13. Emsley P and Cowtan K. Coot: model-building tools for molecular graphics. *Acta Crystallogr D Biol Crystallogr* 60: 2126–2132, 2004.
14. Frova C. Glutathione transferases in the genomics era: new insights and perspectives. *Biomol Eng* 23: 149–169, 2006.
15. Grauschopf U, Winther JR, Korber P, Zander T, Dallinger P, and Bardwell JC. Why is DsbA such an oxidizing disulfide catalyst? *Cell* 83: 947–955, 1995.
16. Grimshaw JP, Stirnimann CU, Brozzo MS, Malojcic G, Grutter MG, Capitani G, and Glockshuber R. DsbL and DsbI form a specific dithiol oxidase system for periplasmic arylsulfate sulfotransferase in uropathogenic *Escherichia coli*. *J Mol Biol* 380: 667–680, 2008.
17. Guddat LW, Bardwell JC, and Martin JL. Crystal structures of reduced and oxidized DsbA: investigation of domain motion and thiolate stabilization. *Structure* 6: 757–767, 1998.
18. Guddat LW, Bardwell JC, Zander T, and Martin JL. The uncharged surface features surrounding the active site of *Escherichia coli* DsbA are conserved and are implicated in peptide binding. *Protein Sci* 6: 1148–1156, 1997.
19. Guddat LW, Bardwell JC, Glockshuber R, Huber-Wunderlich M, Zander T, and Martin JL. Structural analysis of three His32 mutants of DsbA: support for an electrostatic role of His32 in DsbA stability. *Protein Sci* 6: 1893–1900, 1997.
20. Guzman LM, Belin D, Carson MJ, and Beckwith J. Tight regulation, modulation, and high-level expression by vectors containing the arabinose PBAD promoter. *J Bacteriol* 177: 4121–4130, 1995.
21. Haworth NL, Gready JE, George RA, and Wouters MA. Evaluating the stability of disulfide bridges in proteins: a torsional potential energy surface for diethyl disulfide. *Mol Simul* 33: 475–485, 2007.
22. Heras B, Kurz M, Shouldice SR, and Martin JL. The name's bond: disulfide bond. *Curr Opin Struct Biol* 17: 691–698, 2007.
23. Heras B, Edeling MA, Schirra HJ, Raina S, and Martin JL. Crystal structures of the DsbG disulfide isomerase reveal an unstable disulfide. *Proc Natl Acad Sci U S A* 101: 8876–8881, 2004.
24. Heras B, Shouldice SR, Totsika M, Scanlon MJ, Schembri M, and Martin JL. Dsb proteins and bacterial pathogenicity. *Nature Rev Microbiol* 7: 215–225, 2009.
25. Heras B, Kurz M, Jarrott R, Shouldice SR, Frei P, Robin G, Cemazar M, Thony-Meyer L, Glockshuber R, and Martin JL. *Staphylococcus aureus* DsbA does not have a destabilizing disulfide: a new paradigm for bacterial oxidative folding. *J Biol Chem* 283: 4261–4271, 2008.
26. Holmgren A. Thioredoxin catalyzes the reduction of insulin disulfides by dithiothreitol and dihydrolipoamide. *J Biol Chem* 254: 9627–9632, 1979.
27. Hu SH, Peek JA, Rattigan E, Taylor RK, and Martin JL. Structure of TcpG, the DsbA protein folding catalyst from *Vibrio cholerae*. *J Mol Biol* 268: 137–146, 1997.
28. Huber-Wunderlich M and Glockshuber R. A single dipeptide sequence modulates the redox properties of a whole enzyme family. *Fold Des* 3: 161–171, 1998.
29. Inaba K, Murakami S, Suzuki M, Nakagawa A, Yamashita E, Okada K, and Ito K. Crystal structure of the DsbB-DsbA complex reveals a mechanism of disulfide bond generation. *Cell* 127: 789–801, 2006.
30. Iturbe-Ormaetxe I and O'Neill SL. *Wolbachia*-host interactions: connecting phenotype to genotype. *Curr Opin Microbiol* 10: 221–224, 2007.
31. Jeyaprakash A and Hoy MA. Long PCR improves *Wolbachia* DNA amplification: wsp sequences found in 76% of sixty-three arthropod species. *Insect Mol Biol* 9: 393–405, 2000.
32. Kadokura H, Nichols L, and Beckwith J. Mutational alterations of the key *cis* proline residue that cause accumulation of enzymatic reaction intermediates of DsbA, a member of the thioredoxin superfamily. *J Bacteriol* 187: 1519–1522, 2005.
33. Krissinel E and Henrick K. Secondary-structure matching (SSM), a new tool for fast protein structure alignment in three dimensions. *Acta Crystallogr D Biol Crystallogr* 60: 2256–2268, 2004.
34. Kurz M, Iturbe-Ormaetxe I, Jarrott R, O'Neill SL, Byriel KA, Martin JL, and Heras B. Crystallization and preliminary diffraction analysis of a DsbA homologue from *Wolbachia pipientis*. *Acta Crystallogr Sect F Struct Biol Cryst Commun* 64: 94–97, 2008.
35. Kurz M, Iturbe-Ormaetxe I, Jarrott R, Cowieson N, Robin G, Jones A, King GJ, Frei P, Glockshuber R, O'Neill SL, Heras B, and Martin JL. Cloning, expression, purification and characterization of a DsbA-like protein from *Wolbachia pipientis*. *Protein Expr Purif* 59: 266–273, 2008.
36. Li H, Singh AK, McIntyre LM, and Sherman LA. Differential gene expression in response to hydrogen peroxide and the

putative PerR regulon of *Synechocystis* sp. strain PCC 6803. *J Bacteriol* 186: 3331–3345, 2004.
37. Li Y, Hu Y, Zhang X, Xu H, Lescop E, Xia B, and Jin C. Conformational fluctuations coupled to the thiol-disulfide transfer between thioredoxin and arsenate reductase in *Bacillus subtilis*. *J Biol Chem* 282: 11078–11083, 2007.
38. Lin TY and Kim PS. Urea dependence of thiol-disulfide equilibria in thioredoxin: confirmation of the linkage relationship and a sensitive assay for structure. *Biochemistry* 28: 5282–5287, 1989.
39. Maeda K, Hagglund P, Finnie C, Svensson B, and Henriksen A. Structural basis for target protein recognition by the protein disulfide reductase thioredoxin. *Structure* 14: 1701–1710, 2006.
40. Martin JL. Thioredoxin: a fold for all reasons. *Structure* 3: 245–250, 1995.
41. Martin JL, Bardwell JC, and Kuriyan J. Crystal structure of the DsbA protein required for disulphide bond formation *in vivo*. *Nature* 365: 464–468, 1993.
42. McMeniman CJ, Lane RV, Cass BN, Fong AW, Sidhu M, Wang YF, and O'Neill SL. Stable introduction of a life-shortening *Wolbachia* infection into the mosquito *Aedes aegypti*. *Science* 323: 141–144, 2009.
43. Messens J and Collet JF. Pathways of disulfide bond formation in *Escherichia coli*. *Int J Biochem Cell Biol* 38: 1050–1062, 2006.
44. Morris RJ, Perrakis A, and Lamzin VS. ARP/wARP and automatic interpretation of protein electron density maps. *Methods Enzymol* 374: 229–244, 2003.
45. Nelson JW and Creighton TE. Reactivity and ionization of the active site cysteine residues of DsbA, a protein required for disulfide bond formation *in vivo*. *Biochemistry* 33: 5974–5983, 1994.
46. Otwinowski Z and Minor W. Processing of X-ray diffraction data collected in oscillation mode. *Methods Enzymol* 276: 307–326, 1997.
47. Pearlman D, Case D, Caldwell J, Ross W, Cheatham T, Debolt S, Ferguson D, Seibel G, and Kollman P. AMBER, a computer program for applying molecular mechanics, normal mode analysis, molecular dynamics and free energy calculations to elucidate the structures and energies of molecules. *Comp Phys Commun* 91: 1–41, 1995.
48. Ren G, Stephan D, Xu Z, Zheng Y, Tang D, Harrison RS, Kurz M, Jarrott R, Shouldice SR, Hiniker A, Martin JL, Heras B, and Bardwell JC. Properties of the thioredoxin fold superfamily are modulated by a single amino acid residue. *J Biol Chem* 284: 10150–10159, 2009.
49. Riegler M and O'Neill SL. The genus *Wolbachia*. In: *The Prokaryotes*, 3rd ed., edited by Dworkin M, Falkow S, Rosenberg E, Schleifer KH, and Stackebrandt E. New York: Springer Science, 2006, pp. 547–561.
50. Sun XX and Wang CC. The N-terminal sequence (residues 1-65) is essential for dimerization, activities, and peptide binding of *Escherichia coli* DsbC. *J Biol Chem* 275: 22743–22749, 2000.
51. Terwilliger T. SOLVE and RESOLVE: automated structure solution, density modification, and model building. *J Synchr Rad* 11: 49–52, 2004.
52. Thurlkill RL, Grimsley GR, Scholtz JM, and Pace CN. pK values of the ionizable groups of proteins. *Protein Sci* 15: 1214–1218, 2006.
53. Tian G, Xiang S, Noiva R, Lennarz WJ, and Schindelin H. The crystal structure of yeast protein disulfide isomerase suggests cooperativity between its active sites. *Cell* 124: 61–73, 2006.
54. Vivian J, Scoullar J, Robertson A, Bottomley S, Horne J, Chin Y, Wielens J, Thompson P, Velkov T, Piek S, Byres E, Beddoe T, Wilce M, Kahler C, Rossjohn J, and Scanlon M. Structural and biochemical characterisation of the oxidoreductase NmDsbA3 from *Neisseria meningitidis*. *J Biol Chem* 283: 32452–32461, 2008.
55. Weik M, Ravelli RB, Kryger G, McSweeney S, Raves ML, Harel M, Gros P, Silman I, Kroon J, and Sussman JL. Specific chemical and structural damage to proteins produced by synchrotron radiation. *Proc Natl Acad Sci U S A* 97: 623–628, 2000.
56. Werren JH and O'Neill SL. The evolution of heritable symbionts. In: *Influential passengers: inherited microorganisms and arthropod reproduction*., edited by O'Neill SL, Hoffmann AA, and Werren JH. Oxford, UK: Oxford University Press, 1997, pp. 1–41.
57. Wouters MA, George RA, and Haworth NL. "Forbidden" disulfides: their role as redox switches. *Curr Protein Pept Sci* 8: 484–495, 2007.
58. Wu M, Sun LV, Vamathevan J, Riegler M, Deboy R, Brownlie JC, McGraw EA, Martin W, Esser C, Ahmadinejad N, Wiegand C, Madupu R, Beanan MJ, Brinkac LM, Daugherty SC, Durkin AS, Kolonay JF, Nelson WC, Mohamoud Y, Lee P, Berry K, Young MB, Utterback T, Weidman J, Nierman WC, Paulsen IT, Nelson KE, Tettelin H, O'Neill SL, and Eisen JA. Phylogenomics of the reproductive parasite *Wolbachia pipientis* w*Mel*: a streamlined genome overrun by mobile genetic elements. *PLoS Biol* 2: 327–341, 2004.
59. Wunderlich M, Jaenicke R, and Glockshuber R. The redox properties of protein disulfide isomerase (DsbA) of *Escherichia coli* result from a tense conformation of its oxidized form. *J Mol Biol* 233: 559–566, 1993.
60. Zapun A, Missiakas D, Raina S, and Creighton TE. Structural and functional characterization of DsbC, a protein involved in disulfide bond formation in *Escherichia coli*. *Biochemistry* 34: 5075–5089, 1995.

Address reprint requests to:
Jennifer L. Martin
Institute for Molecular Bioscience
The University of Queensland
QLD 4072, Australia

E-mail: j.martin@imb.uq.edu.au and b.heras@imb.uq.edu.au

Date of first submission to ARS Central, December 23, 2008; date of final revised submission, March 1, 2009; date of acceptance, March 5, 2009.

This article has been cited by:

1. Katleen Denoncin , Jean-François Collet . Disulfide Bond Formation in the Bacterial Periplasm: Major Achievements and Challenges Ahead. *Antioxidants & Redox Signaling*, ahead of print. [Abstract] [Full Text HTML] [Full Text PDF] [Full Text PDF with Links]
2. Patricia M. Walden, Begoña Heras, Kai-En Chen, Maria A. Halili, Kieran Rimmer, Pooja Sharma, Martin J. Scanlon, Jennifer L. Martin. 2012. The 1.2 Å resolution crystal structure of TcpG, the Vibrio cholerae DsbA disulfide-forming protein required for pilus and cholera-toxin production. *Acta Crystallographica Section D Biological Crystallography* **68**:10, 1290-1302. [CrossRef]
3. Merridee A. Wouters, Siiri Iismaa, Samuel W. Fan, Naomi L. Haworth. 2011. Thiol-based redox signalling: Rust never sleeps. *The International Journal of Biochemistry & Cell Biology* **43**:8, 1079-1085. [CrossRef]
4. Richard Glatz, Joanne Kent. 2011. Insect molecular biology: an Australian perspective. *Australian Journal of Entomology* no-no. [CrossRef]
5. Stephen R. Shouldice , Begoña Heras , Patricia M. Walden , Makrina Totsika , Mark A. Schembri , Jennifer L. Martin . 2011. Structure and Function of DsbA, a Key Bacterial Oxidative Folding Catalyst. *Antioxidants & Redox Signaling* **14**:9, 1729-1760. [Abstract] [Full Text HTML] [Full Text PDF] [Full Text PDF with Links]
6. Stephen R. Shouldice , Begoña Heras , Russell Jarrott , Pooja Sharma , Martin J. Scanlon , Jennifer L. Martin . 2010. Characterization of the DsbA Oxidative Folding Catalyst from Pseudomonas aeruginosa Reveals a Highly Oxidizing Protein that Binds Small Molecules. *Antioxidants & Redox Signaling* **12**:8, 921-931. [Abstract] [Full Text HTML] [Full Text PDF] [Full Text PDF with Links]
7. Martin L. Williams, David K. Chalmers, Jennifer L. Martin, Martin J. Scanlon. 2010. Backbone and side chain 1H, 15N and 13C assignments for the oxidised and reduced forms of the oxidoreductase protein DsbA from Staphylococcus aureus. *Biomolecular NMR Assignments* **4**:1, 25-28. [CrossRef]
8. Julian P. Vivian, Jessica Scoullar, Kieran Rimmer, Simon R. Bushell, Travis Beddoe, Matthew C.J. Wilce, Emma Byres, Tristan P. Boyle, Bradley Doak, Jamie S. Simpson. 2009. Structure and Function of the Oxidoreductase DsbA1 from Neisseria meningitidis. *Journal of Molecular Biology* **394**:5, 931-943. [CrossRef]
9. K. Inaba. 2009. Disulfide Bond Formation System in Escherichia coli. *Journal of Biochemistry* **146**:5, 591-597. [CrossRef]